Supporting Information

Insights into Photocatalytic Selective Dehydrogenation of Ethanol over Au/Anatase−Rutile TiO_2

Sifan Jia, Xin Shu, Hongyan Song, Zhe An, Xu Xiang, Jian Zhang, Yanru Zhu and Jing He**

State Key Laboratory of Chemical Resource Engineering & Beijing Advanced Innovation Center for Soft Matter Science and Engineering, Beijing University of Chemical Technology, Beijing 100029, P. R. China

*Corresponding Author E-mail:

shuxin@mail.buct.edu.cn

hejing@mail.buct.edu.cn or jinghe@263.net.cn

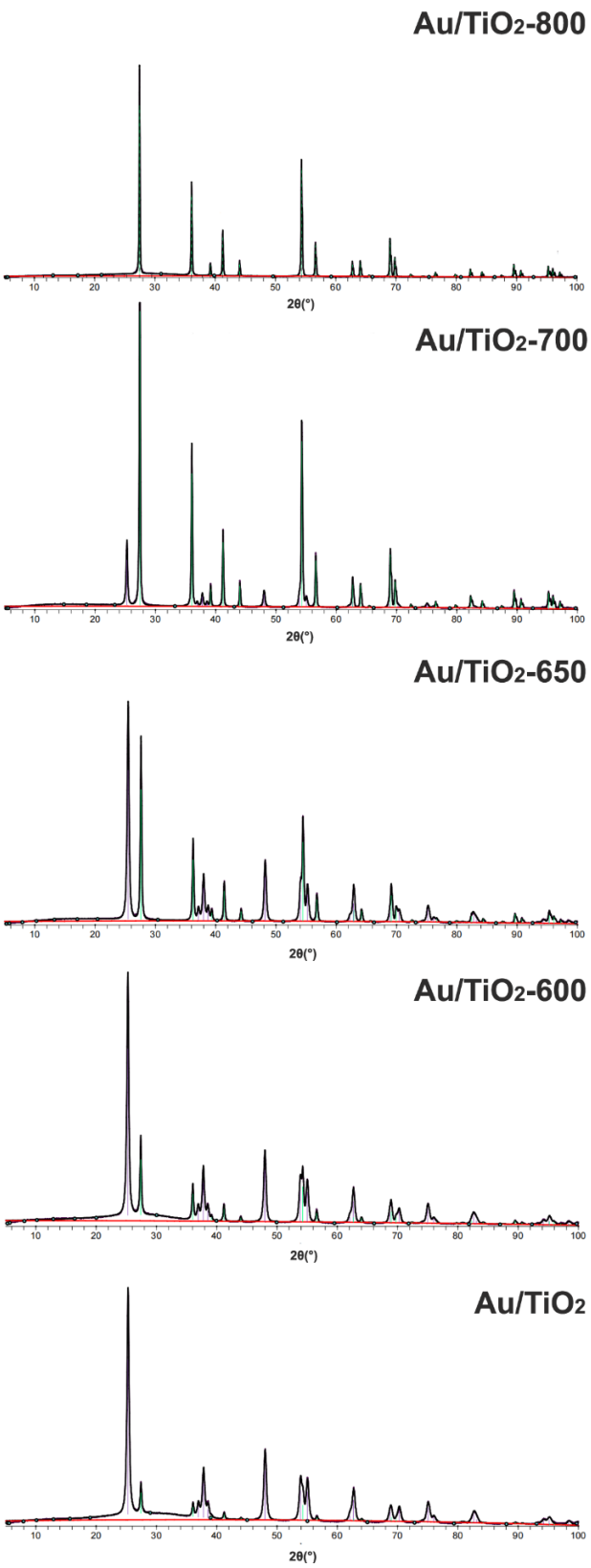

Figure S1. Rietveld refinement fitting to powder X-ray diffraction data for Au/TiO_2-*x*.

Table S1. Comparison of calculation methods of rutile TiO_2 composition

entry	catalyst	composition of rutile TiO_2 (%)	
		Rietveld refinement method	*k* value method
1	Au/TiO_2	10.4	7.8
2	Au/TiO_2-600	20.3	17.7
3	Au/TiO_2-650	42.0	42.8
4	Au/TiO_2-700	73.1	78.8
5	Au/TiO_2-800	100	100

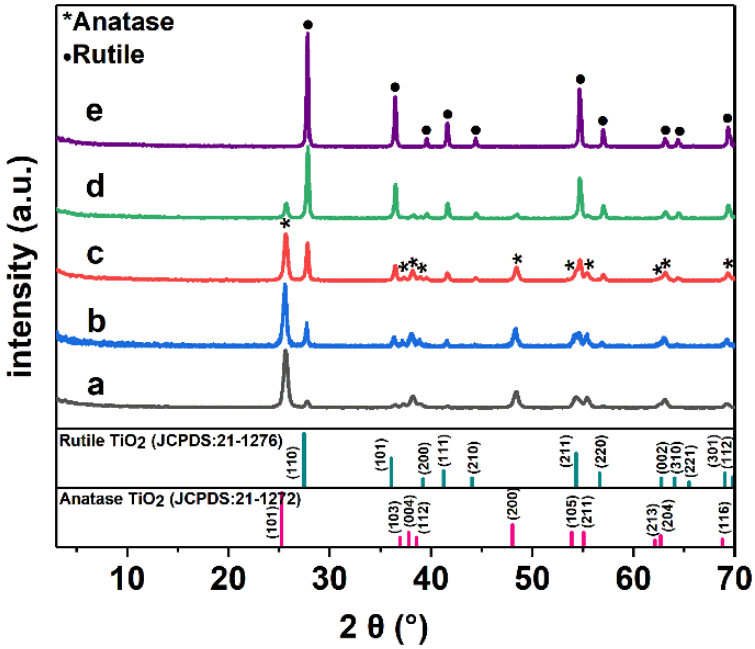

Figure S2. XRD patterns of (a) TiO_2, (b) TiO_2-600, (c) TiO_2-650, (d) TiO_2-700 and (e) TiO_2-800.

Table S2. Specific surface area and TiO_2 particle size of TiO_2 and Au/TiO_2

entry	catalyst	S_{BET} (m^2/g)	TiO_2 particle size (nm)	
			anatase	rutile
1	TiO_2	42.2	20.5	28.1
2	TiO_2-600	41.8	23.7	31.2
3	TiO_2-650	38.9	26.7	35.6
4	TiO_2-700	22.7	27.3	35.0
5	TiO_2-800	4.9	-	76.1
6	Au/TiO_2	41.5	21.2	28.3
7	Au/TiO_2-600	40.2	24.4	32.0
8	Au/TiO_2-650	38.1	26.8	36.0
9	Au/TiO_2-700	21.3	27.5	34.7
10	Au/TiO_2-800	4.8	-	75.2

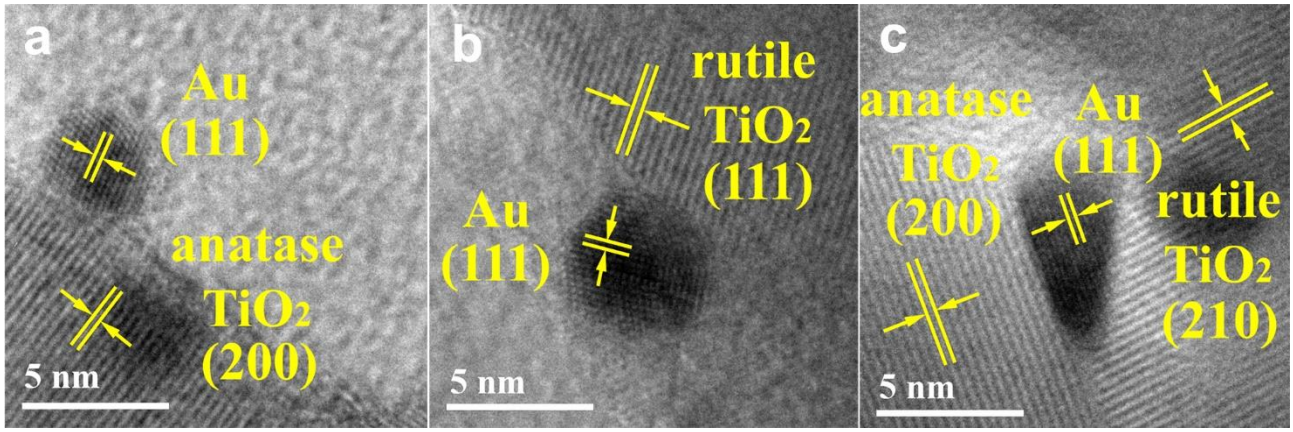

Figure S3. HRTEM images of Au nanoparticles of (a) Au/anatase TiO_2, (b) Au/rutile TiO_2 and (c)Au/anatase−rutile TiO_2 for Au/TiO_2-650.

Table S3. Catalytic performance with different concentration of reactants

entry	catalyst	concentration of ethanol and Benzotrifluoride	con. (%)	sel. (mol %)		
				acetaldehyde	1,1-diethoxyethane	ethyl formate
1	Au/TiO_2-650	1: 9	48.7 (48.1)	2.4 (2.6)	93.1 (92.8)	4.5 (4.6)
2	Au/TiO_2-650	2: 8	47.5	3.1	91.2	5.7
3	Au/TiO_2-650	3: 7	43.2	1.9	92.7	5.4
4	Au/TiO_2-800	1: 9	11.9 (12.3)	- (-)	95.9 (95.7)	4.1 (4.3)
5	Au/TiO_2-800	2: 8	11.7	-	96.2	3.8
6	Au/TiO_2-800	3: 7	9.3	-	95.6	4.4

[a] Reaction conditions: 0.3 g of photocatalysts, N_2 atmosphere, UV-light irradiation, T=20 °C, t=6 h. Calculated C balance (mol%) > 90 %.

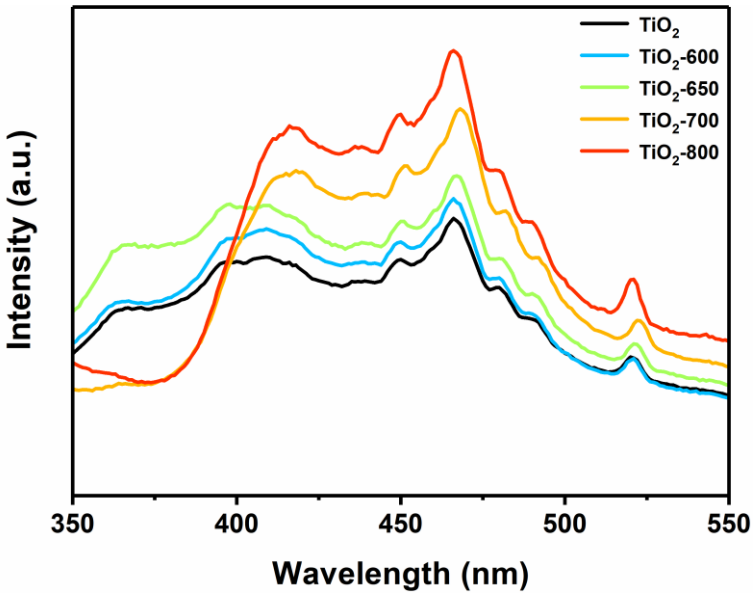

Figure S4. PL spectra of TiO_2-*x* samples.

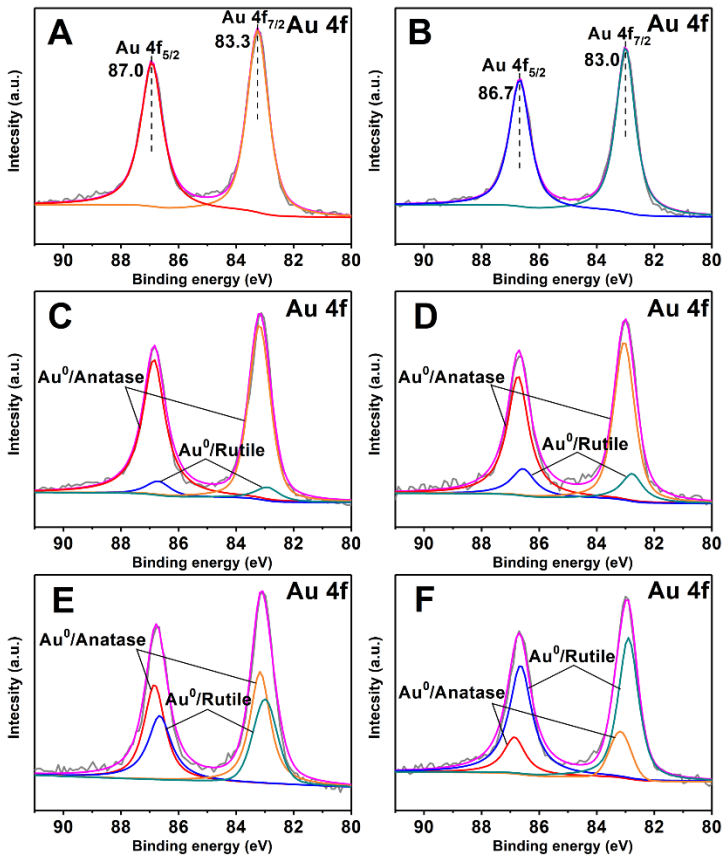

Figure S5. Au 4f XPS spectra of (A) Au/anatase TiO_2, (B) Au/rutile TiO_2, (C) Au/TiO_2, (D) Au/TiO_2-600, (E) Au/TiO_2-650 and (F) Au/TiO_2-700.

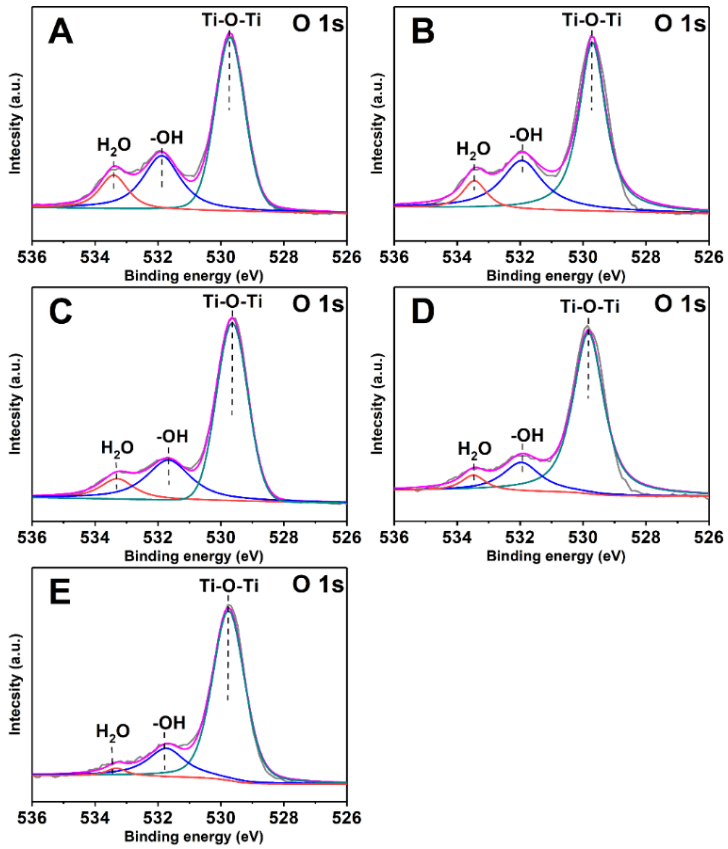

Figure S6. O 1s XPS spectra of (A) Au/TiO_2, (B) Au/TiO_2-600, (C) Au/TiO_2-650, (D) Au/TiO_2-700 and (E) Au/TiO_2-800.

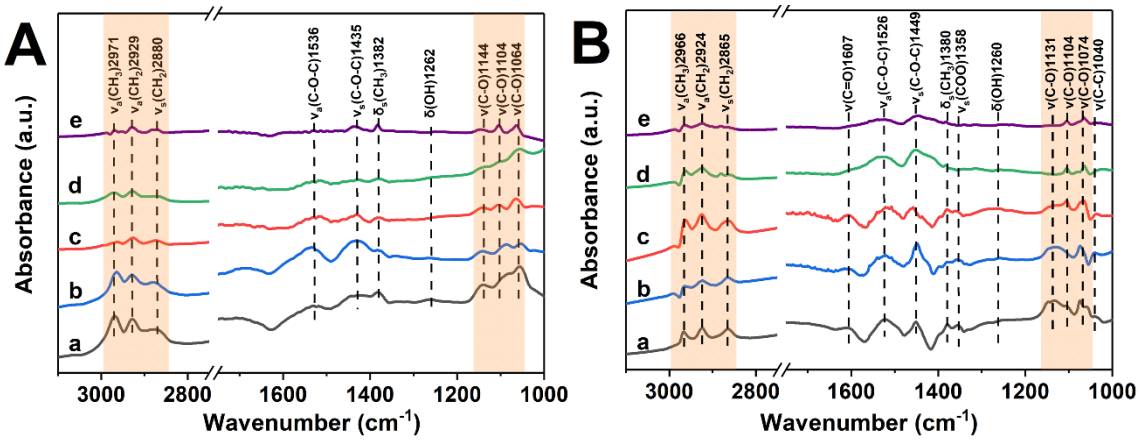

Figure S7. (A) In situ FT-IR spectra of ethanol adsorption at 20 °C under UV irradiation on (a) TiO_2, (b) TiO_2-600, (c) TiO_2-650, (d) TiO_2-700 and (e) TiO_2-800. (B) In situ FT-IR spectra of ethanol adsorption at 20 °C under UV irradiation on (a) Au/TiO_2, (b) Au/TiO_2-600, (c) Au/TiO_2-650, (d) Au/TiO_2-700 and (e) Au/TiO_2-800.

Table S4. Band assignments and their vibration modes on Au/TiO_2

species	bands (cm^{-1}) and modes
$C_2H_5OH_{ad}$	$\nu_a(CH_3)$/2966, $\nu_a(CH_2)$/2924, $\nu_s(CH_2)$/2865, $\delta_s(CH_3)$/1380, δ(OH)/1260, ν(C−O)/1074, ν(C−C)/1040
$C_2H_5O_{ad}$	$\nu_a(CH_3)$/2966, $\nu_a(CH_2)$/2924, $\nu_s(CH_2)$/2865, ν(C−O) monodentate/1131 and 1104, ν(C-O) bidentate/1074
η^1-CH_3CHO	ν(C=O)/1607
CH_3COO^-	ν_a(O−C−O)/1526, ν_s(O−C−O)/1449
$HCOO^-$	ν_s(COO)/1358

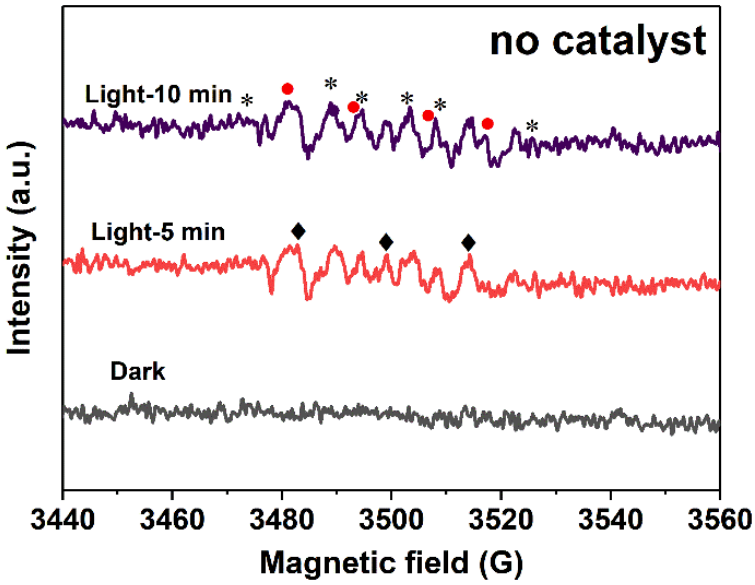

Figure S8. EPR spectra recorded during the irradiation of sample with no catalyst. DMPO−$CH_3CH(OH)$• (aN=14.94, aH=21.48, g=2.0063) marked as * and DMPO−CH_3CH_2O• (aN=13.59, aH=7.65, aH=1.72, g=2.0063) marked as ●, signals marked as ♦ belong to the existing oxidation product of DMPO, 5,5-dimethyl-2-oxopyrroline-1-oxyl (DMPOX).

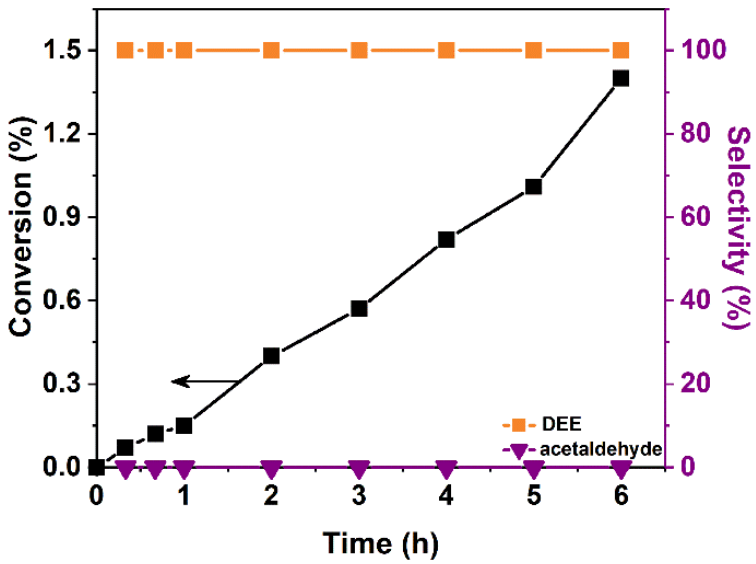

Figure S9. The conversion of ethanol and the selectivity of products as a function of the reaction time of sample with no catalyst.